

APP-BP1 mediates APP-induced apoptosis and DNA synthesis and is increased in Alzheimer's disease brain

Yuzhi Chen, Wenyun Liu, Donna L. McPhie, Linda Hassinger, and Rachael L. Neve

Department of Psychiatry, Harvard Medical School, McLean Hospital, Belmont, MA 02478

APP-BP1, first identified as an amyloid precursor protein (APP) binding protein, is the regulatory subunit of the activating enzyme for the small ubiquitin-like protein NEDD8. We have shown that APP-BP1 drives the S- to M-phase transition in dividing cells, and causes apoptosis in neurons (Chen, Y., D.L. McPhie, J. Hirschberg, and R.L. Neve. 2000. *J. Biol. Chem.* 275: 8929–8935). We now demonstrate that APP-BP1 binds to the COOH-terminal 31 amino acids of APP (C31) and colocalizes with APP in a lipid-enriched fraction called lipid rafts. We show that coexpression of a peptide representing the domain of APP-BP1 that binds to APP, abolishes the ability of overexpressed APP or the V642I mutant of APP to

cause neuronal apoptosis and DNA synthesis. A dominant negative mutant of the NEDD8 conjugating enzyme hUbc12, which participates in the ubiquitin-like pathway initiated by APP-BP1, blocks neuronal apoptosis caused by APP, APP(V642I), C31, or overexpression of APP-BP1. Neurons overexpressing APP or APP(V642I) show increased APP-BP1 protein levels in lipid rafts. A similar increase in APP-BP1 in lipid rafts is observed in the Alzheimer's disease brain hippocampus, but not in less-affected areas of Alzheimer's disease brain. This translocation of APP-BP1 to lipid rafts is accompanied by a change in the subcellular localization of the ubiquitin-like protein NEDD8, which is activated by APP-BP1.

Introduction

The mechanism by which neurons die in Alzheimer's disease (AD) remains to be defined. However, the participation of the amyloid precursor protein (APP) in at least some aspects of the etiology of the disease is suggested by the facts that mutations in this gene can cause familial AD (FAD) and that APP is overexpressed in Down's syndrome, a disorder that culminates in AD-like neurodegeneration. Therefore, it is useful to understand the normal function of APP, as impairments of its function may contribute to AD neuropathology. For example, cleavage of APP by β - and γ -secretases not only generates the pathological amyloid β (A β) peptide but also releases an intracellular fragment (APP intracellular cleavage domain [AICD]) that can cause apoptosis in neuroglioma cells (Kinoshita et al., 2002).

A subset of total APP is found on the cell surface in neurons (Jung et al., 1996), suggesting that a percentage of APP may function as a cell surface receptor, transducing signals from the ECM to the interior of the cell. Consistent with this notion, a number of proteins have been shown to interact with the COOH-terminal, intracellular portion of APP, among them the growth cone G protein G_o (Nishimoto et

al., 1993), the presumptive adaptor proteins Fe65 and X11 (for review see Russo et al., 1998), UV-DDB (Watanabe et al., 1999), histone acetyltransferase Tip60 (Cao and Sudhof, 2001), and Jun NH₂-terminal kinase interaction protein 1 (Scheinfeld et al., 2002).

Previously, we identified an additional binding protein for the intracellular domain of APP, APP-BP1 (Chow et al., 1996). We showed that APP-BP1 is a cell cycle protein that acts in vivo as one half of the bipartite activating enzyme for the ubiquitin-like protein NEDD8 (Chen et al., 2000). Expression of APP-BP1 in dividing cells drives the cell cycle through the S-M checkpoint; this function is mediated by the NEDD8 conjugation (neddylation) pathway. In primary neurons, overexpression of APP-BP1 causes apoptosis; this apoptosis can be blocked by inhibition of neddylation (Chen et al., 2000).

Here, we dissect the nature of the interaction of APP-BP1 with APP, to determine whether disruptions in this interaction may play a role in AD neurodegeneration. We show that APP-BP1 binds to the COOH-terminal 31 aa of APP (C31), and that both proteins are located in lipid rafts. We demonstrate that APP, as well as APP-BP1, overexpression

Address correspondence to Yuzhi Chen, MRC 223, McLean Hospital, 115 Mill St., Belmont, MA 02478. Tel.: (617) 855-3627. Fax: (617) 855-3793. email: ychen@helix.mgh.harvard.edu

Key words: APP(V642I); NEDD8; secretase; lipid rafts; cell cycle

Abbreviations used in this paper: A β , amyloid β ; AD, Alzheimer's disease; AICD, APP intracellular cleavage domain; APP, amyloid precursor protein; FAD, familial AD; WT, wild-type.

causes DNA synthesis and apoptosis in neurons, and that interaction of APP with APP-BP1 is required for activation of these pathways. Inhibition of neddylation blocks neuronal apoptosis caused not only by overexpression of APP-BP1 and APP but also by the V642I mutation of APP and by C31. Neurons expressing APP or APP(V642I) show an increase in APP-BP1 levels in lipid rafts, which is also observed in AD hippocampus. The increase in APP-BP1 is accompanied by a change in the subcellular localization of the ubiquitin-like protein NEDD8, which is activated by APP-BP1.

Results and discussion

APP-BP1 interacts with the COOH-terminal

31 aa of APP

APP-BP1 was first identified as a protein that interacts with the intracellular domain of APP (Chow et al., 1996). We performed coimmunoprecipitations to identify with greater specificity the region of APP to which APP-BP1 binds. Primary rat cortical cells were infected with HSV vectors expressing APP-BP1 and myc epitope-tagged C31. Myc-C31 was immunoprecipitated from the neuronal cell lysates with 9E10, an antibody specific for the myc epitope. As shown in Fig. 1 A, APP-BP1 coprecipitated with myc-C31 in the presence but not in the absence of the primary antibody, indicating that APP-BP1 binds to the C31 of APP. C31, which is generated by intracellular caspase cleavage, causes apoptosis in neuronal cells (Lu et al., 2000; Galvan et al., 2002) and is responsible for the apoptosis caused by FAD mutants of APP (McPhie et al., 2001). The binding of APP-BP1 to C31 suggests involvement of APP-BP1 in neuronal apoptosis caused by this fragment.

APP-BP1 and APP colocalize to lipid rafts

APP has been reported to localize to the detergent-insoluble and lipid-enriched low density fraction (lipid rafts). To determine whether APP-BP1 colocalizes with APP in lipid rafts, we fractionated rat brain homogenates (Chen and Norkin, 1999) and used immunoblots to detect the fractions in which APP and APP-BP1 were enriched. As shown in Fig. 1 B, both APP and APP-BP1 are greatly enriched in fractions 5 and 6, which contain lipid rafts. Our data showing colocalization of APP with APP-BP1 in lipid rafts suggest that not only APP processing but also APP signaling mediated by APP-BP1 may occur in the lipid rafts.

HSV-APP-induced apoptosis and DNA synthesis are blocked by coexpression of a peptide that competes with APP-BP1 for binding to APP

We have shown previously that either overexpression of wild-type (WT) APP or expression of FAD mutants of APP in neurons induces apoptosis and DNA synthesis (McPhie et al., 2001, 2003). To determine whether APP-BP1 interaction with APP is involved in either of these pathways, we used HSV vectors to coexpress in neurons a peptide representing the domain of APP-BP1 that binds to APP (Chow et al., 1996; Chen et al., 2000), together with WT APP or APP(V642I). Fig. 2 (A and B) shows that expression of this peptide, APP-BP1(145-251), blocks neuronal apoptosis and

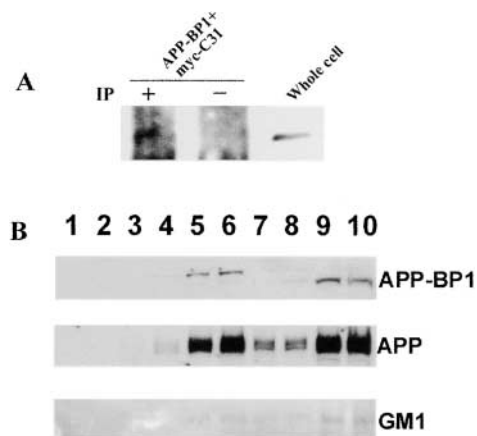
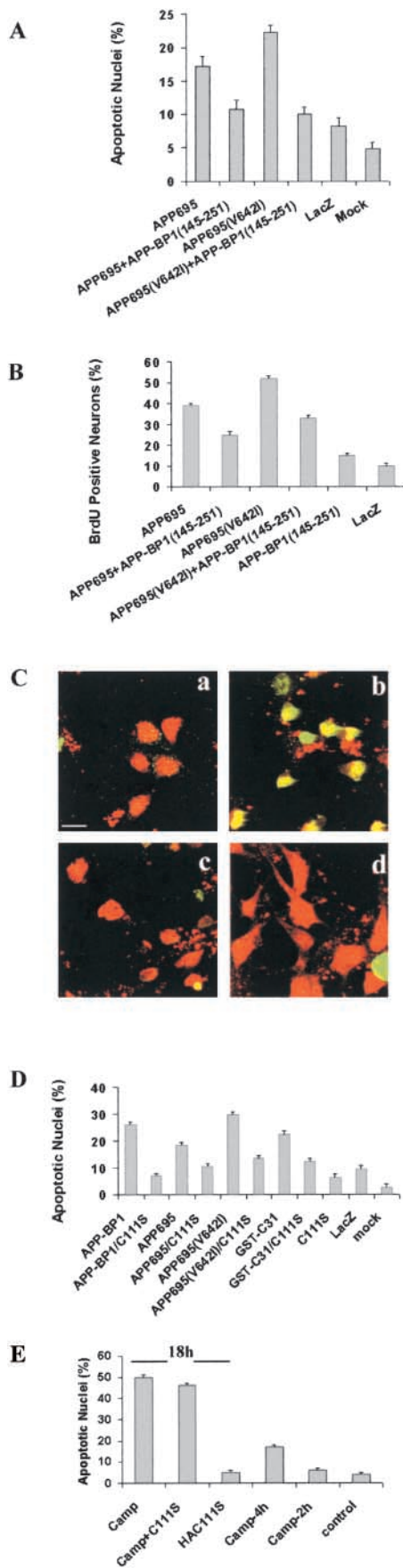


Figure 1. APP-BP1 interacts with APP-C31 in lipid rafts. (A) Primary neurons were infected with HSV vectors expressing APP-BP1 and myc-C31. Myc-C31 was precipitated from the cell lysate with the anti-myc antibody 9E10. The blot was probed with the anti-APP-BP1 antibody BP339. The plus and minus signs indicate presence or absence of the primary antibody, respectively, in the immunoprecipitation. APP-BP1 coprecipitated with myc-C31, but when no primary antibody was present, APP-BP1 was not coprecipitated. The lane labeled "whole cell" represents 4% of the lysate used for immunoprecipitation. (B) Adult rat brain was fractionated to isolate lipid rafts; the ganglioside GM1, detected by HRP-conjugated cholera toxin, was used as a marker for the lipid rafts. APP-BP1 was detected with the rabbit antibody BP339, and APP with the rabbit antibody 369. Both APP-BP1 and APP were enriched in the lipid raft low density fractions (lanes 5 and 6). The image was captured with the imaging system from Imaging Research, Inc. using the MCID software.

DNA synthesis caused by WT APP or APP(V642I), suggesting that interaction of APP with APP-BP1 is required for the activation of these pathways.

Consistent with our previous data (McPhie et al., 2001, 2003), neuronal apoptosis and DNA synthesis caused by overexpression of WT APP is intermediate between that seen in control and that caused by APP(V642I) (Fig. 2, A and B). This is not surprising because we have reported that expression of FAD APP mutants in neurons results in greater accumulation of the β -secretase cleavage product of APP (C99) than does overexpression of WT APP in neurons (McPhie et al., 1997). C99 is a preferred substrate for production of both AICD (Passer et al., 2000) and C31 (Lu et al., 2000), and has been shown to be increased in AD brain (Holsinger et al., 2002; Yang et al., 2003). C99 is also a substrate for the production of the A β fragment, which has been shown to be toxic to neurons in culture. However, our prior data (McPhie et al., 2001) show that neuronal apoptosis caused by FAD mutants of APP is independent of A β production by these mutants indicating that A β caused neurotoxicity is likely to involve a separate pathway from that mediated by APP-BP1.

Fig. 2 C illustrates the increase in DNA synthesis caused by APP(V642I), showing incorporation of BrdU into the DNA of neurons infected with HSV-APP(V642I). To confirm that the increase in DNA synthesis caused by APP(V642I) and blocked by APP-BP1(145-251) occurs specifically in neurons, we stained the neurons with a monoclonal anti-NeuN antibody, specific for neuronal nuclei, together with a polyclonal anti-BrdU antibody. As shown in Fig. 2 C (b), cells that are



positively immunolabeled with anti-BrdU are colabeled with the antibody to NeuN, verifying their identity as neurons.

The fact that APP-BP1 apparently mediates APP-induced neuronal DNA synthesis is not unexpected, given our previous finding that APP-BP1 is necessary for cell cycle progression (Chen et al., 2000). However, in neurons this entry into the cell cycle causes apoptosis rather than cell cycle progression. The induction of DNA synthesis in neurons by overexpression of WT APP or of APP(V642I) is consistent with the data reported by Yang et al. (2001), who demonstrated that a significant number of hippocampal pyramidal and basal forebrain neurons in AD brain compared with control brain have undergone full or partial DNA replication.

APP-induced neuronal apoptosis is antagonized by disruption of the neddylation pathway that is initiated by APP-BP1

Overexpression of APP-BP1 in primary neurons causes apoptosis by a pathway that also involves hUbc12, the NEDD8-conjugating enzyme in the neddylation pathway initiated by APP-BP1. Coexpression of a dominant negative

Figure 2. WT APP- and APP(V642I)-induced neuronal apoptosis and DNA synthesis are inhibited by coexpression of a peptide that competes with APP-BP1 for binding to APP or by blockade of the APP-BP1 neddylation pathway.

(A) Apoptosis induced by overexpression of HSV-APP or HSV-APP(V642I) is inhibited by coinfection with an HSV vector expressing HA-tagged APP-BP1(145-251), which competes with APP-BP1 for binding to APP. A two-tailed *t* test revealed significant differences between APP versus APP + APP-BP1(145-251) ($P < 0.001$) and between APP(V642I) versus APP(V642I) + APP-BP1(145-251) ($P < 0.001$). APP-BP1(145-251) versus LacZ is not significant. (B) Neuronal DNA synthesis induced by HSV-APP or HSV-APP(V642I) is inhibited by coinfection with an HSV vector expressing HA-tagged APP-BP1(145-251), which competes with APP-BP1 for binding to APP. A two-tailed *t* test revealed significant differences between APP versus APP + APP-BP1(145-251) and between APP(V642I) versus APP(V642I) + APP-BP1(145-251) ($P < 0.001$). APP-BP1(145-251) versus LacZ is not significant. (C) DNA synthesis induced by APP(V642I) and blocked by APP-BP1(145-251) is primarily neuronal. Rat cortical cultures were infected with HSV vectors and labeled with BrdU. Cells were fixed and stained with rabbit polyclonal anti-BrdU plus Alexa 488-conjugated secondary (green) and the neuron-specific mouse monoclonal anti-NeuN plus Cy5-conjugated secondary (red). Double-labeled cells represent neurons undergoing DNA synthesis. The four panels represent neuronal cultures infected with the following vectors: (a) HSV-HA-APP-BP1(145-251); and (b) HSV-APP(V642I). Double-labeled neurons were present, showing APP(V642I)-induced DNA synthesis in neurons; (c) HSV-HA-APP-BP1(145-251) plus HSV-APP(V642I); the peptide was able to block DNA synthesis induced by APP(V642I); and (d) Mock. Bar, 10 μm. (D) A dominant negative mutant (C111S) of hUbc12, the NEDD8-conjugating enzyme in the neddylation pathway initiated by APP-BP1, blocks apoptosis induced by APP-BP1, APP, APP(V642I), or GST-C31. A two-tailed *t* test revealed the following significant differences: APP-BP1 versus APP-BP1 + C111S ($P < 0.001$), APP versus APP + C111S ($P < 0.01$), APP(V642I) versus APP(V642I) + C111S ($P < 0.01$), and GST-C31 versus GST-C31 + C111S ($P < 0.001$). (E) A dominant negative mutant (C111S) of hUbc12 does not block apoptosis induced by treatment of neurons with 10 μM camptothecin (Camp). A two-tailed *t* test revealed the following significant differences: Camp-18 h versus control and Camp-4 h versus control ($P < 0.001$). Camp-18 h versus Camp+C111S and Camp-2 h versus control were not significant. All error bars represent SEM.

mutant (C111S) of hUbc12 with APP-BP1 prevents APP-BP1-mediated neuronal apoptosis (Chen et al., 2000). We asked whether hUbc12(C111S) also blocks APP-induced apoptosis in neurons. As shown in Fig. 2 D, coexpression of hUbc12(C111S) with HSV-APP or with HSV-APP(V642I) reduces apoptosis induced by these viral recombinants nearly to control levels.

We suggested previously (McPhie et al., 2001) that APP C31 is responsible for the apoptosis caused by FAD mutants of APP. Therefore, we asked whether apoptosis caused by C31 is mediated by the neddylation pathway. Neurons in culture were infected with HSV vectors expressing GST-tagged C31 alone or in combination with hUbc12(C111S). The results (Fig. 2 D) confirm that C31 directly causes neuronal apoptosis, and that this apoptosis is inhibited by dominant negative hUbc12. Thus, activation of the neddylation pathway mediates neuronal apoptosis caused by APP-BP1, WT APP, APP(V642I), and C31.

To ascertain whether the dominant negative mutant of hUbc12 has a general effect on apoptotic pathways, we tested the effect of expression of hUbc12 dominant negative mutant on neurons treated with camptothecin, a topoisomerase inhibitor that activates the G1 to S transition in neurons and causes neuronal apoptosis (Park et al., 1997). Camptothecin induced a significant increase in DNA fragmentation in cortical cells; this effect peaked at 18 h (Fig. 2 E). This increase in DNA fragmentation was not prevented by coinfection with HSV expressing the dominant negative mutant of hUbc12 (Fig. 2 E). These data suggest either that camptothecin acts in a distinct apoptotic pathway or that its effects on apoptosis are distal to the effect of APP-BP1 in the same pathway.

The data above support the idea that APP-BP1 interaction with APP signals cells to divide via the neddylation pathway, causing differentiated neurons to die.

Expression of FAD APP(V642I) in neurons causes increased expression of APP-BP1 in the Triton X-100-insoluble fraction

We have demonstrated that overexpression of APP-BP1 causes apoptosis in neurons. These data suggest that WT or FAD APPs may initiate the apoptotic pathway at least partly by increasing the level of APP-BP1 in neurons. To test this hypothesis, levels of APP-BP1 were assayed in lysates of neurons that had been infected with HSV-APP or HSV-APP(V642I) (Fig. 3 A). When primary cortical cultures were infected with these recombinant viruses, the level of the endogenous APP-BP1 in the Triton X-100-insoluble/SDS-soluble fraction (lipid rafts) was increased many fold over basal levels. Expression of WT APP in neurons caused an intermediate increase in APP-BP1 levels in lipid rafts, consistent with our previous observation that overexpression of APP in neurons causes a level of DNA synthesis and apoptosis intermediate between that caused by APP(V642I) and that seen in control cultures. Camptothecin did not cause an increase of APP-BP1 in lipid rafts (Fig. 3 B); in fact, it caused a decrease, suggesting again that it acts by a different pathway from that activated by APP. No differences in total cellular APP-BP1 levels were detected in the samples shown

in Fig. 3 (A and B; not depicted). These data suggest that WT APP and APP(V642I) cause the activation of cell cycle machinery and consequent apoptosis in neurons by increasing APP-BP1 levels specifically in lipid rafts.

APP-BP1 protein levels are increased in Triton X-100-insoluble compartments of hippocampal cells in postmortem AD brain

Our observation that overexpression of WT APP and APP(V642I) in neurons causes an increase in APP-BP1 protein in the Triton X-100-insoluble fraction suggests that APP-BP1 protein might also be increased in AD brain in the same fraction. Therefore, we performed immunoblot analyses of hippocampal tissue samples from postmortem AD and control brains (Fig. 3 C). Equal amounts of Triton X-100-insoluble proteins from each sample were analyzed with the anti-APP-BP1 antibody BP339. Densitometric analysis of the blots showed that levels of APP-BP1 were significantly increased in AD hippocampus relative to control hippocampus (Fig. 3 C, b).

Immunofluorescent staining of Triton X-100-treated hippocampal tissue sections with BP339 (Fig. 3 D) showed increased APP-BP1 in pyramidal cells in the hippocampus, supporting the immunoblot results. Brodmann areas 9 and 17, less pathologically affected in AD, were also analyzed by immunoblot, and did not show elevated levels of APP-BP1 over those in the same regions of control brain (Fig. 3 E). We did not observe increased APP-BP1 protein levels in the hippocampus of Parkinson's disease brains relative to controls (Fig. 3 F).

NEDD8 is translocated to the cytoplasm in hippocampal neurons in AD brain and in cultured neurons overexpressing APP-BP1

NEDD8 is a small ubiquitin-like protein that is activated by APP-BP1/hUba3 and covalently conjugated to target proteins such as the cullins. During most phases of the cell cycle, NEDD8 is located predominantly in the nucleus, but as mitosis begins, it moves to a predominantly cytoplasmic location (Kurz et al., 2002). Given that WT APP and APP(V642I) cause neuronal DNA synthesis that is mediated by APP-BP1, we predicted that NEDD8 may show a shift from a neuronal to a cytoplasmic localization in affected regions of AD brain. Indeed, we did observe such a shift (Fig. 4 A). We immunostained the hippocampus in five cases of AD and five matching controls with rabbit anti-NEDD8. In four out of five AD cases examined, NEDD8 was located primarily in the cytoplasm in hippocampal neurons. In contrast, in four out of five control cases, NEDD8 was located primarily in the nucleus in hippocampal neurons. Although the postmortem interval average for the control cases was slightly longer than that for the AD cases (average of 20 ± 1.28 h vs. 15 ± 1.96 h), there was no correlation between postmortem interval and NEDD8 localization in the cases that were examined. These data reinforce the notion that neurons in AD brain may be entering the cell cycle, and support the observation by Yang et al. (2001) that a significant number of hippocampal pyramidal and basal forebrain neurons in AD brain compared with control brain have undergone full or partial DNA replication.

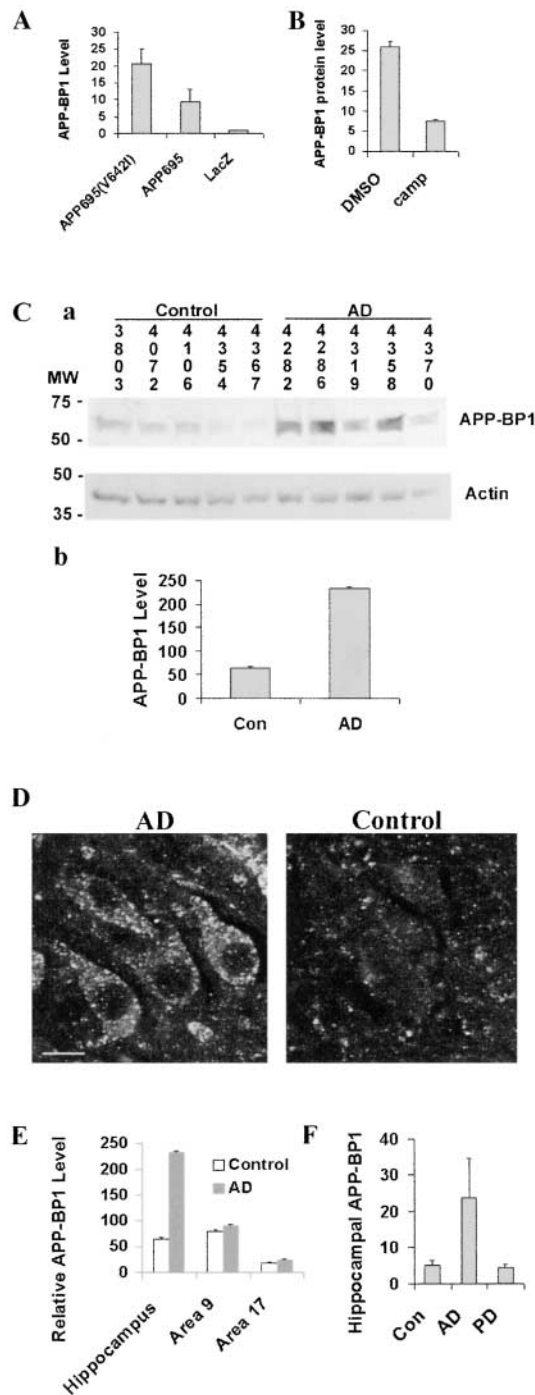


Figure 3. APP-BP1 levels in lipid rafts are increased in primary neurons overexpressing APP or APP(V642I) and in AD hippocampus.

(A) Triton X-100-insoluble fractions from HSV-infected primary neurons were analyzed by immunoblot expression for endogenous APP-BP1 protein expression. APP-BP1 was up-regulated in the HSV-APP- and HSV-APP(V642I)-infected neurons, but not in the HSV-LacZ-infected neurons. The experiment was repeated three times. The density of APP-BP1 for each sample was first normalized to actin, and then calculated as fold of LacZ (LacZ = 1). Error bars represent SEM for three independent experiments. (B) Triton X-100-insoluble fractions from primary neurons treated with 10 μ M camptothecin (camp) or vehicle (DMSO) were analyzed by immunoblot expression for endogenous APP-BP1 protein expression. APP-BP1 levels in the lipid rafts were down-regulated by camptothecin. The density of APP-BP1 for each sample was normalized to actin. Error

bars represent SEM for two independent experiments. (C) Frozen postmortem human brain tissue was homogenized, and protein from the Triton X-100-insoluble fraction was analyzed by immunoblotting with the anti-APP-BP1 antibody BP339 (a). Densitometric analysis of the immunoblot data (b), in which the APP-BP1 signal was normalized to the actin signal, revealed a significant difference between APP-BP1 levels in control (Con) and AD hippocampus, by two-tailed *t* test ($P = 0.026$). Error bars represent SEM after APP-BP1 levels were normalized to actin. (D) PFA-fixed human hippocampal tissue sections were immunostained in the presence of Triton X-100 with the anti-APP-BP1 antibody BP339 plus Alexa 488-conjugated secondary antibody. APP-BP1 immunofluorescence was visualized by confocal microscopy, using the same settings for each case. CA2 pyramidal cells are shown. Bar, 20 μ m. (E) APP-BP1 protein levels in the Triton X-100-insoluble fraction from Brodmann areas 9 and 17 are not significantly different in AD brain from their levels in control brain. For the analysis of APP-BP1 in the hippocampus and area 17, nine AD and nine control cases were used. For the area 9 analysis, eight AD and eight control cases were used. The APP-BP1 signal was normalized to that for actin. Error bars represent SEM after APP-BP1 levels were normalized to actin. (F) APP-BP1 is expressed at higher levels in AD hippocampus than in the Parkinson's disease hippocampus. Equal amounts of protein from the Triton X-100-insoluble fraction, two cases from each category, were analyzed. The APP-BP1 signal was normalized to that for actin. Error bars represent SD after APP-BP1 levels were normalized to actin.

Conclusions

In summary, APP-BP1 interacts with APP within the COOH-terminal 31 aa of APP, and the two proteins coexist in lipid rafts. Induction of apoptosis or DNA synthesis in neurons by overexpression of wild type APP or APP(V642I) depends on the interaction of APP with APP-BP1 and is blocked by inhibition of neddylation. The levels of endogenous APP-BP1 protein in lipid rafts are both increased by APP or APP(V642I) overexpression in primary neuronal cultures and also increased in AD hippocampus. This increase in APP-BP1 levels in lipid rafts is associated with the translocation of NEDD8 from the nucleus to the cytoplasm both in AD hippocampal neurons and in primary neuronal cultures.

Our data suggest that neuronal apoptosis induced by overexpression of APP is mediated by its interaction with APP-BP1 in lipid rafts, which activates the neddylation pathway and induces cell cycle entry. It has been reported previously

bars represent SEM for two independent experiments. (C) Frozen postmortem human brain tissue was homogenized, and protein from the Triton X-100-insoluble fraction was analyzed by immunoblotting with the anti-APP-BP1 antibody BP339 (a). Densitometric analysis of the immunoblot data (b), in which the APP-BP1 signal was normalized to the actin signal, revealed a significant difference between APP-BP1 levels in control (Con) and AD hippocampus, by two-tailed *t* test ($P = 0.026$). Error bars represent SEM after APP-BP1 levels were normalized to actin. (D) PFA-fixed human hippocampal tissue sections were immunostained in the presence of Triton X-100 with the anti-APP-BP1 antibody BP339 plus Alexa 488-conjugated secondary antibody. APP-BP1 immunofluorescence was visualized by confocal microscopy, using the same settings for each case. CA2 pyramidal cells are shown. Bar, 20 μ m. (E) APP-BP1 protein levels in the Triton X-100-insoluble fraction from Brodmann areas 9 and 17 are not significantly different in AD brain from their levels in control brain. For the analysis of APP-BP1 in the hippocampus and area 17, nine AD and nine control cases were used. For the area 9 analysis, eight AD and eight control cases were used. The APP-BP1 signal was normalized to that for actin. Error bars represent SEM after APP-BP1 levels were normalized to actin. (F) APP-BP1 is expressed at higher levels in AD hippocampus than in the Parkinson's disease hippocampus. Equal amounts of protein from the Triton X-100-insoluble fraction, two cases from each category, were analyzed. The APP-BP1 signal was normalized to that for actin. Error bars represent SD after APP-BP1 levels were normalized to actin.

that the AICD, to which APP-BP1 binds, causes neuronal apoptosis via its effects on transcription (Kinoshita et al., 2002). One clue to the connection between APP-BP1 and the transcriptional pathway activated by the AICD is suggested by the finding that activation of NF- κ B inhibits the transcriptional activity of AICD (Zhao and Lee, 2003). We have shown that the neddylation pathway inhibits NF- κ B activation (Chen et al., 2003). One may infer from these findings that activation of the neddylation pathway by APP-BP1 antagonizes the inhibition of the transcriptional activity of

AICD by NF- κ B, resulting in increased AICD transcriptional activity.

Materials and methods

Primary rat cortical culture and HSV infection

For apoptosis and DNA synthesis assays, primary cortical cultures from E17/18 rat embryos were plated at a density of 3.5×10^5 viable cells per 35-mm well containing poly-D-lysine-coated glass coverslips. 4–5 d after plating, neurons were infected with the appropriate viruses at a multiplicity of infection of one per virus. In experiments in which two different viruses were coexpressed, HSV-LacZ was added to the conditions involving expression of single viruses, to equalize the amount of virus in all conditions.

Plasmid construction

All plasmid constructs were made in the pHSVPrpUC vector or in the pcDNA3 vector using standard techniques, and were verified by sequence analysis. The APP-BP1 and dominant negative hUbc12 HSV vectors have been described previously (Chen et al., 2000), as have been the APP-695, APP(V642I), and myc-C31 HSV vectors (McPhie et al., 1997, 2001).

Antibodies and immunoblots

The polyclonal antibody 369, raised against amino acids 645–694 of human APP₆₉₅, was a gift from S. Gandy (Thomas Jefferson University, Phila-

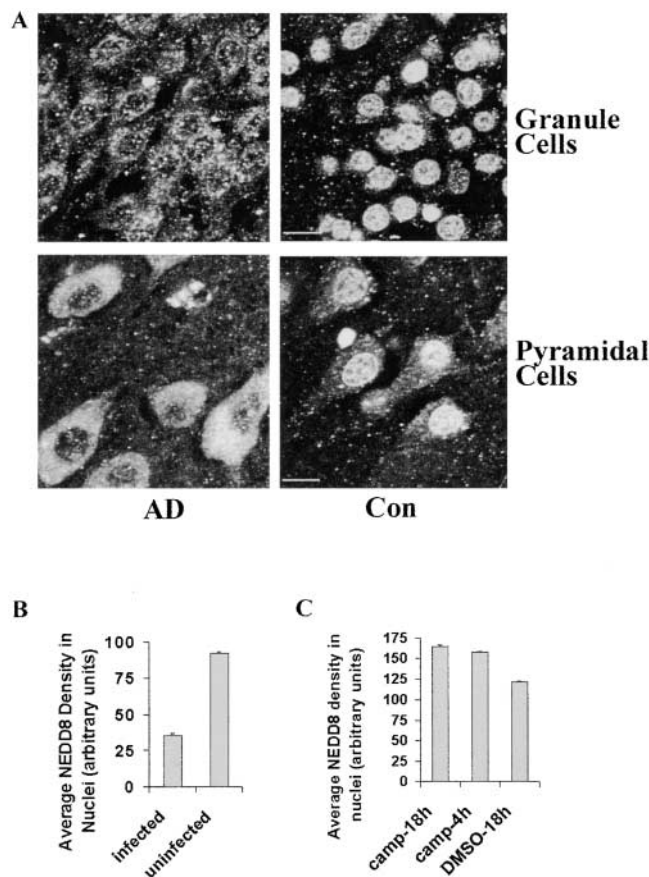


Figure 4. NEDD8 shows a shift from the nucleus to the cytoplasm in AD hippocampal neurons and in cultured neurons overexpressing APP-BP1. (A) PFA-fixed human postmortem brain sections were immunostained with rabbit anti-NEDD8. Confocal microscopic images of NEDD8 immunofluorescence in CA2 pyramidal cells and granule cells were visualized. Bar, 20 μ m. (B) Primary neuronal cultures were infected with HSV-myc-APP-BP1. 4 h later, cells were fixed with 4% PFA and immunostained with mouse anti-myc antibody 9E10 (1:400; visualized with Alexa Fluor 488 goat anti-mouse), and 10 μ g/ml rabbit anti-NEDD8 (visualized with Cy5 goat anti-rabbit). Cell nuclei were counterstained with 50 μ g/ml propidium iodide (Sigma-Aldrich) for 5 min. The density of NEDD8 in the nuclei of HSV-myc-APP-BP1-infected versus uninfected neurons on the same slide was quantified with confocal software (Leica); the difference was shown to be significant ($P < 0.0001$). (C) Primary neuronal cultures were treated with 10 μ M camptothecin (camp) for 4 or 18 h, or with vehicle (DMSO) for 18 h. Either 4 or 18 h of camptothecin treatment caused an increase in the density of NEDD8 in the nuclei of neurons versus the vehicle control ($P < 0.001$). All error bars represent SEM.

Table I. Summary of human brain materials used

Brain type	Case	PMI	Age	Sex	Pathology grade
		<i>h</i>			
Control	3803	25	81	M	mild AD changes
	4072	21	69	F	mild AD changes
	4106	19	74	M	mild AD changes
	4354	15	68	F	
	4367	26	75	F	
	4481	20	65	M	
	4646	22	68	F	
	4722	26	60	M	mild AD changes
	4571	24	71	M	
	4585	22	59	M	mild AD changes
	4595	17	65	M	
	4298	22	75	F	
	4320	15	62	M	^a
	4343	5	76	M	mild AD changes ^a
4393	18	70	F	^a	
4596	25	49	M	^a	
4480	18	57	M	^a	
Alzheimer's disease	4282	13	65	M	4
	4286	20	69	F	2 genetic
	4319	23	84	M	4 ^a
	4358	18	73	F	2 ^a
	4370	25	74	F	2
	4152	7	63	M	3
	4559	14	61	F	3
	4495	5	67	M	2
4639	24	67	M	1	
4233	14	73	F	3 ^a	
4336	16	76	F	3 ^a	
4342	3	73	F	3	
4420	13	68	M	2 ^a	
Parkinson's disease	4078	12	72	F	
	4934	17	68	M	

^aCases used for immunocytochemistry.

delphia, PA). The anti-myc antibody 9E10 and the anti-APP antibody 22C11 were both obtained from CHEMICON International, Inc. or Upstate Biotechnology. The anti-APP-BP1 antibody BP339 has been described previously (Chen et al., 2000). The other antibodies used include: rabbit polyclonal anti-BrdU (Megabase Research Products); mouse monoclonal anti-NeuN (CHEMICON International, Inc.); Cy5-conjugated secondary (Jackson ImmunoResearch Laboratories); 10 μ g/ml of rabbit anti-NEDD8 (Qbiogene or Zymed Laboratories); and myc antibody 9E10 (1:400; CHEMICON International, Inc.). HRP-conjugated cholera toxin, propidium iodide and (S)-(+)-camptothecin all were obtained from Sigma-Aldrich. Immunoblots were performed as described previously (Chen et al., 2000).

Coimmunoprecipitation

Rat primary neurons were infected with HSV-APP-BP1 and HSV myc-C31 for 4 h. Coimmunoprecipitation was performed as described previously (McPhie et al., 2003). The lysate was incubated with the anti-myc antibody 9E10 overnight and then with protein G for 2 h. The immune complex was resolved by SDS-PAGE, and subjected to immunoblot analysis with anti-APP-BP1 antibody BP339.

Apoptosis and DNA synthesis assays

For apoptosis assays, primary cortical cultures were infected with the appropriate viruses at a multiplicity of infection of one, and 14 h later, the cells were fixed for 20 min with 4% PFA and stained with bisbenzimidazole as described previously (McPhie et al., 2001). 10 random fields of 100–200 cells were analyzed for each condition. The number of cells with condensed nuclei relative to the total number of cells per field was calculated and expressed as a percentage. All experiments were repeated three to four times. Both the DNA synthesis assays and the statistical analyses have been described in detail in Chen et al. (2003).

Immunocytochemistry with postmortem human brain sections and with ethanol-fixed primary neurons

40- μ m-thick postmortem brain tissues fixed in PFA (Table I; Harvard Brain Tissue Resource Center) were immersed in TBS (20 mM Tris, pH 7.4, and 8.75% NaCl), rinsed three times with 10 mM phosphate buffer, and twice with diluting buffer (10 mM phosphate containing 2% BSA, 0.4% Triton X-100, and 1% normal goat serum). The tissue sections were incubated in 20% normal goat serum in 10 mM phosphate buffer for 10 min, after which they were incubated with rabbit anti-APP-BP1, BP339, or with rabbit anti-NEDD8 at room temperature for 40 h. Sections were washed once in 10 mM phosphate buffer and twice in diluting buffer. The sections were incubated with Alexa Fluor goat anti-rabbit overnight and washed before they were mounted onto slides.

Confocal images in Fig. 2 (B and C), Fig. 3 D, and Fig. 4 were all collected with the confocal system (model TCS SP2; Leica) using the confocal software (LCS; Leica; 40 \times ; NA 1.25; zoom 1 \times). In Fig. 3 D, APP-BP1 immunofluorescence was visualized by confocal microscopy, using the same settings for each case. In Fig. 4 B, images were collected in three channels.

We thank Dr. Anne Cataldo for helpful discussions.

This work was supported by National Institutes of Health grant AG12954 to R.L. Neve. Y. Chen is an American Health Assistance Foundation Investigator for Alzheimer's Disease Research.

Submitted: 1 April 2003

Accepted: 28 August 2003

References

Cao, X., and T.C. Sudhof. 2001. A transcriptionally [correction of transcriptively] active complex of APP with Fe65 and histone acetyltransferase Tip60. *Science*. 293:115–120.

Chen, Y., and L.C. Norkin. 1999. Extracellular simian virus 40 transmits a signal that promotes virus enclosure within caveolae. *Exp. Cell Res.* 246:83–90.

Chen, Y., D.L. McPhie, J. Hirschberg, and R.L. Neve. 2000. The amyloid precursor protein-binding protein APP-BP1 drives the cell cycle through the S-M checkpoint and causes apoptosis in neurons. *J. Biol. Chem.* 275:8929–8935.

Chen, Y., W. Liu, L. Naumovski, and R.L. Neve. 2003. ASP2 Inhibits APP-BP1-mediated NEDD8 conjugation to Cullin-1 and decreases APP-BP1-induced cell proliferation and neuronal apoptosis. *J. Neurochem.* 85:801–809.

Chow, N., J.R. Korenberg, X.N. Chen, and R.L. Neve. 1996. APP-BP1, a novel protein that binds to the carboxyl-terminal region of the amyloid precursor protein. *J. Biol. Chem.* 271:11339–11346.

Galvan, V., S. Chen, D. Lu, A. Logvinova, P. Goldsmith, E.H. Koo, and D.E. Bredesen. 2002. Caspase cleavage of members of the amyloid precursor family of proteins. *J. Neurochem.* 82:283–294.

Holsinger, R.M.D., A. Catriona, M.D. McLean, K. Beyreuther, C.L. Masters, and G. Evin. 2002. Increased expression of the amyloid precursor β -secretase in Alzheimer's disease. *Ann. Neurol.* 51:783–786.

Jung, S.S., J. Nalbantoglu, and N.R. Cashman. 1996. Alzheimer's β -amyloid precursor protein is expressed on the surface of immediately ex vivo brain cells: a flow cytometric study. *J. Neurosci. Res.* 46:336–348.

Kinoshita, A., C.M. Whelan, O. Berezovska, and B.T. Hyman. 2002. The γ secretase-generated carboxyl-terminal domain of the amyloid precursor protein induces apoptosis via Tip60 in H4 cells. *J. Biol. Chem.* 277:28530–28536.

Kurz, T., L. Pintard, J.H. Willis, D.R. Hamill, P. Gonczy, M. Peter, and B. Bowerman. 2002. Cytoskeletal regulation by the Nedd8 ubiquitin-like protein modification pathway. *Science*. 295:1294–1298.

Lu, D.C., S. Rabizadeh, S. Chandra, R.F. Shayya, L.M. Ellerby, X. Ye, G.S. Salvesen, E.H. Koo, and D.E. Bredesen. 2000. A second cytotoxic proteolytic peptide derived from amyloid β -protein precursor. *Nat. Med.* 6:397–404.

McPhie, D.L., R.K.K. Lee, C.B. Eckman, D.H. Olstein, S.P. Durham, D. Yager, S.G. Younkin, R.J. Wurtman, and R.L. Neve. 1997. Neuronal expression of β -amyloid precursor protein Alzheimer mutations causes intracellular accumulation of a C-terminal fragment containing both the amyloid β and cytoplasmic domains. *J. Biol. Chem.* 272:24743–24746.

McPhie, D.L., T. Golde, C.B. Eckman, D. Yager, J.B. Brant, and R.L. Neve. 2001. β -Secretase cleavage of the amyloid precursor protein mediates neuronal apoptosis caused by familial Alzheimer's disease mutations. *Brain Res. Mol. Brain Res.* 97:103–113.

McPhie, D.L., R. Coopersmith, A. Hines-Peralta, Y. Chen, K.J. Ivins, S.P. Manly, M.R. Kozlowski, K.A. Neve, and R.L. Neve. 2003. DNA synthesis and neuronal apoptosis caused by familial Alzheimer's disease mutants of the amyloid precursor protein are mediated by the p21 activated kinase PAK3. *J. Neurosci.* 23:6914–6927.

Nishimoto, I., T. Okamoto, Y. Matsuura, S. Takahashi, T. Okamoto, Y. Murayama, and E. Ogata. 1993. Alzheimer amyloid protein precursor complexes with brain GTP-binding protein G(o). *Nature*. 362:75–79.

Park, D.S., E.J. Morris, L.A. Greene, and H.M. Geller. 1997. G1/S cell cycle blockers and inhibitors of cyclin-dependent kinases suppress camptothecin-induced neuronal apoptosis. *J. Neurosci.* 17:1256–1270.

Passer, B., L. Pellegrini, C. Russo, R.M. Siegel, M.J. Lenardo, G. Schettini, M. Bachmann, M. Tabaton, and L. D'Adamio. 2000. Generation of an apoptotic intracellular peptide by γ -secretase cleavage of Alzheimer's amyloid β protein precursor. *J. Alzheimers Dis.* 2:289–301.

Russo, T., R. Faraonio, G. Minopoli, P. De Candia, S. De Renzis, and N. Zambano. 1998. Fe65 and the protein network centered around the cytosolic domain of the Alzheimer's β -amyloid precursor protein. *FEBS Lett.* 434:1–7.

Scheinfeld, M.H., R. Roncarati, P. Vito, P.A. Lopez, M. Abdallah, and L. D'Adamio. 2002. Jun NH2-terminal kinase (JNK) interacting protein 1 (JIP1) binds the cytoplasmic domain of the Alzheimer's beta-amyloid precursor protein (APP). *J. Biol. Chem.* 277:3767–3775.

Watanabe, T., J. Sukegawa, I. Sukegawa, S. Tomita, K. Iijima, S. Oguchi, T. Suzuki, A.C. Nairn, and P. Greengard. 1999. A 127-kDa protein (UV-DDB) binds to the cytoplasmic domain of the Alzheimer's amyloid precursor protein. *J. Neurochem.* 72:549–556.

Yang, L.-B., K. Lindholm, R. Yan, M. Citron, W. Weiming, X.-L. Yang, T. Beach, L. Sue, P. Wong, D. Price, et al. 2003. Elevated β -secretase expression and enzymatic activity detected in sporadic Alzheimer disease. *Nat. Med.* 9:3–4.

Yang, Y., D.S. Geldmacher, and K. Herrup. 2001. DNA replication precedes neuronal cell death in Alzheimer's disease. *J. Neurosci.* 21:2661–2668.

Zhao, Q., and F.S. Lee. 2003. The transcriptional activity of the APP intracellular domain-Fe65 complex is inhibited by activation of the NF- κ B pathway. *Biochemistry*. 42:3627–3634.